Mathematical Biosciences and Engineering

MBE, 16(6): 7155–7176.
DOI: 10.3934/mbe.2019359
Received: 30 April 2019
Accepted: 28 July 2019
Published: 07 August 2019

http://www.aimspress.com/journal/MBE

Research article

Modal identification of a high-rise building subjected to a landfall typhoon via both deterministic and Bayesian methods

Yuncheng He, Zhen Liu, Zhi Li, Jiurong Wu and Jiyang Fu*

Joint Research Center for Engineering Structure Disaster Prevention and Control, Guangzhou University Guangdong 510006, China

*** Correspondence:** Email: jiyangfu@gzhu.edu.cn; Tel: +8602039366003.

Abstract: Modal identification involves primarily the determination of natural frequencies, damping ratios, mode shapes of a dynamic system, etc. It is usually regarded as an essential task in a wide branch of structural dynamics and civil engineering, such as structural vibration control and damage identification of buildings or bridges. There are many modal identification techniques. Basically, these techniques can be categorized into two groups: deterministic methods and Bayesian approaches. The first group can be used to provide deterministic (or optimal) estimations of modal parameters, but they are unable to quantify the estimation uncertainties. The second group is based on a usage of the Bayesian framework. Compared to the first group, the second group of methods has a typical merit of being able to offer uncertainty information of identified parameters, which is of great interests, or even necessary, for some follow-up studies. In this paper, both a deterministic method, i.e., a combination of spectral analysis, filtering and Random Decrement Technique (RDT), and a Bayesian method, i.e., Bayesian Spectral Density Approach (BSDA), are exploited to experimentally identify the modal parameters of a 303 m high-rise building that was subjected to a landfall typhoon. The validity and efficiency of each method is verified by comparing the two kinds of results. Meanwhile, the identified modal parameters are used for the serviceability assessment of this high-rise building against some frequency-specific criteria.

Keywords: modal identification; Bayesian approach; deterministic method; high-rise building; typhoon

1. Introduction

Modal parameters (i.e., natural frequency, ratio damping, mode shape, etc.) index the inherent properties of a dynamic system, by which the dynamic characteristics of the system can be quantified and predicted. Thus, modal analysis is normally recognized as one of the most important tasks in a wide branch of structural mechanics, such as finite element model (FEM) updating, fault diagnosis and health monitoring of civil structures.

During the last decades, numerous large-scale civil structures have been constructed, including high-rise buildings and long-span bridges. These structures take a significant role in the social and economic developments. Therefore, their safety and serviceability have received great concerns at both the design and maintain stages. For related engineering practices, it is essential to identify the modal parameters of these structures effectively. For example, to restrain the wind-induced vibration of a super-tall building via a tuned-mass-damper (TMD) system, one has first to identify the fundamental natural frequency of the building accurately so that the pendulum length of the TMD system can be determined [1,2].

There are many modal identification techniques. Basically, these techniques can be categorized into two groups: deterministic methods and Bayesian approaches. The first group can be used to provide deterministic (or optimal) estimations of modal parameters. According to the working conditions, the deterministic methods can be further divided into experimental modal analysis (EMA) methods, and operational modal analysis (OMA) methods. An EMA method is conventionally established on the basis of the frequency response function (FRF) of the dynamic system under an experimental working condition. It requires both the input and output information of the system. Unfortunately, it is usually quite expensive or even unfeasible in practices to get the output and input records simultaneously. By contrast, an OMA method identifies the modal parameters of a system under an operational condition (e.g., a building excited by wind load), typically based on output-only records. Since there are no special requirements of input records, using OMA methods for modal analysis becomes considerably economical and convenient. Thus, they have been adopted widely in recent years especially for the cases of large-scale civil structures.

Technically, the OMA methods can be categorized into the following groups: time-domain method, frequency-domain method and time-frequency domain method. The time-domain methods include the auto-regressive-moving-average (ARMA) method [3], random decrement technique (RDT) [4,5], Ibrahim time domain (ITD) method [6], eigensystem realization algorithm (ERA) [7], stochastic subspace identification (SSI) method [8], natural excitation technique (NExT) [9], and least square complex exponential (LSCE) method [10]. The frequency-domain methods are based on spectral analysis of output signals of the dynamic systems, which include peak picking method (PP) [11,12], and frequency domain decomposition (FDD) method [13]. The time-frequency domain methods are developed by using time-frequency domain data analysis techniques, such as wavelet transform [14] and Hilbert-Huang transform (HHT) [15]. They are attractive to deal with problems with non-stationary and/or non-linear features.

Despite the wide utilization of deterministic modal identification methods, there are some limitations for this kind of methods. Typically, they are unable to quantify the estimation uncertainties. It is undoubted that due to the wide existence of noise in measurement records and errors in estimation models or methods, there must be some uncertainty of the modal identification results. Studies have also revealed that the values of modal parameters of civil structures may vary

noticeably with some ambient factors, e.g., temperature [16–19]. Thus, it would be of great interests, or even necessary, to evaluate the estimation uncertainty for some follow-up studies. The Bayesian modal identification methods are established by using a Bayesian analysis framework. Compared to the deterministic methods, this kind of methods are able to offer uncertainty information of identified parameters besides the optimal values of modal parameters.

The pioneering work on modal analysis via Bayesian methods may be traced back to the late of 1990s when Katafygiotis and Beck [20,21] for the first time proposed a modal identification method by using spectral analysis and Bayesian statistical framework to estimate the optimal values of modal parameters based on output-only records of a dynamic system subjected to random excitation. During the past two decades, great developments have been achieved in this researching area. Following the study by Katafygiotis and Beck, Katafygiotis and Yuen [22] proposed a Bayesian spectral density approach (BSDA) which can offer not only the optimal values of modal parameters but also the estimation uncertainty. Later, Yuen [23] proposed the fast Bayesian FFT, which can improve the computational efficiency of Bayesian modal identification methods significantly. Au [24,25] investigated further on the posterior uncertainty of the modal parameters based on the fast Bayesian FFT method. In recent years, many studies have been conducted to use Bayesian methods for modal analysis [26–29].

In this paper, both a deterministic method and a Bayesian method are exploited for the modal analysis of a 303 m high building that was subjected to a landfall typhoon, with a primary objective of examining the working performances of these two kinds of modal identification methods. The involved deterministic method is actually a combination of a series of techniques that include power spectral density (PSD) analysis, filtering and RDT method; while the Bayesian method refers to the BSDA method.

The reminders of this article are organized as follows: Section 2 introduces the adopted methodology which includes two PSD estimation methods, a zero-phase filtering technique and the RDT and BSDA methods. Section 3 states the studied building and datasets. In Section 4, results obtained via the two kinds of methods are presented and compared. The identified modal parameters are further used for the serviceability assessment of this high-rise building against some frequency-specific criterion. Main conclusions are summarized in Section 5.

2. Methodology statement

2.1. Overview of the methodology

Figure 1 illustrates an overview of the methodology adopted in this study. The PSD analysis is conducted first to identify the natural frequencies and frequency bands for each mode of the studied civil structure. Two specific PSD estimation techniques are utilized herein: Welch method and Yule–Walker method. Based on the PSD analysis results, filtering process is manipulated to separate each modal component from the total response, since both the deterministic and Bayesian modal identification methods adopted in this study are only applicable for single-degree-of-freedom (SDOF) cases. Note that the RDT method involved in the deterministic method belongs to a time-domain technique, whose performance may be influenced negatively if the phase information is distorted during the filtering process. To avoid such phase-distortion effects, this study utilizes a zero-phase filtering technique. On obtaining the separated modal responses, the two modal identification methods, i.e., RDT and BSDA, are adopted to determine the modal parameters of the civil structure.

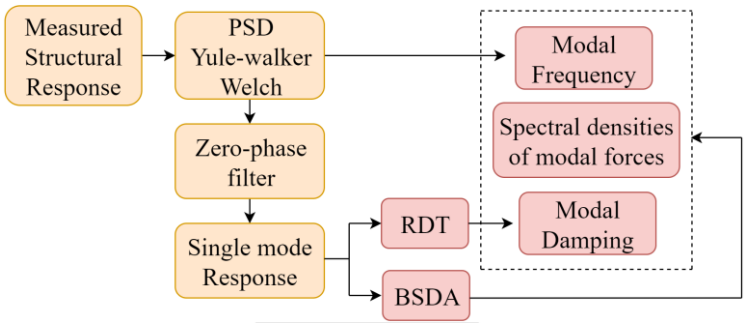

Figure 1. Flowchart of the methodology.

2.2. PSD analysis

There exist many PSD estimation methods. Basically, these methods can be classified into two groups: classic methods and modern methods. The classic methods are principally based on Fourier transform, while the modern methods are established on the basis of parametric models. Two specific PSD estimation methods are considered in this study: the Welch method which belongs to the classic group and the Yule–Walker method which belongs to the modern group.

2.2.1. Welch method

Technologically, the Welch method is a combination of the fast Fourier transform (FFT) and the windowing and averaging techniques. It has been well recognized that analyzing PSD via a pure FFT method usually suffers from severe effects of sidelobe leakage. By bringing in the windowing technique, the sidelobe leakage effects can be suppressed effectively. Meanwhile, by encapsulating the averaging technique into FFT, the obtained results can be improved significantly in terms of the stability of PSD estimations.

Specifically, this method consists of four successive steps: (1) dividing the time series of signals into a pre-assigned number of segments, with the number of samples in each segment uniformly equal to an integral power of 2 so that the FFT can be conducted smoothly; (2) operating windowing process (e.g., using Hanning window) on each segment so that the segmental signals can be smoothed at both edges; (3) estimating PSD for each windowed segment via the so-called periodogram method (which is essentially the same to FFT); (4) calculating the average of PSD results obtained in (3).

It is worthy to note that, although the averaging technique can improve the estimation variance, this improvement is achieved at the price of reducing the number of samples in each segment, which results in a reduction of resolution in the frequency resolution. Thus, special attention is needed so that an acceptable balance between variance inhibition and resolution performance can be obtained [30].

2.2.2. Yule–Walker method

Modern PSD estimators are established by using certain parametric models. Each parametric model can be embodied by a linear system:

$$x(n) \to L(z) \to X(n) \tag{1}$$

where, $x(n)$ denotes the discrete-time signal, $L(z)$ stands for the linear system, or the transfer function of a discrete-time system, $X(n)$ corresponds to the output of $L(z)$ excited by $x(n)$.

The basic idea of modern PSD estimation methods lies in that the PSD of $x(n)$ can be estimated via $L(z)$, while $L(z)$ can be identified based on $X(n)$ or the auto-correlation function of $X(n)$.

Apparently, by contrast to classic PSD estimation methods which assume that signals vanish outside the window range, modern methods use parametric models so that the signals can be treated as if they were infinite in length. Thus, modern methods are able to offer more accurate estimation results at a much finer frequency resolution.

Among numerous modern PSD estimation methods, the Yule–Walker auto-regression (AR) method is one of the most widely utilized ones. This method, which is also called the auto-correlation method, fits an AR model to the windowed input data. It does so by minimizing the forward prediction error in the least squares sense.

Given a signal sequence $x(n)$, the variance of $x(n)$ or the variance of estimations of $x(n)$ via an AR model is given as follows:

$$\text{variance} = \hat{\rho} = \frac{1}{N}\sum_{n=-\infty}^{\infty}\left|x(n)+\sum_{k=1}^{p}a(k)x(n-k)\right|^2 \tag{2}$$

where, N is the length of $x(n)$, $a(k),\ k=1,2,...p$ are coefficients of the p-th order AR model. The unobserved samples of the $x(n)$ process (i.e., samples not in the range $0 \le n \le N-1$) are set as zero in Eq 2.

To obtain the estimations of $a(k)$, one may minimize the prediction error power by differentiating Eq 2 with respect to the real and imaginary parts of $a(k)$:

$$\frac{1}{N}\sum_{n=-\infty}^{\infty}\left(x(n)+\sum_{k=1}^{p}a(k)x(n-k)\right)x^*(n-l)=0,\quad l=1,\ 2,\ ..\tag{3}$$

which can be equally rewritten as a function of autocorrelation function estimates:

$$\hat{r}_p + \hat{R}_p\hat{a} = 0 \tag{4}$$

with the estimators expressed as:

$$\hat{r}(k)=\begin{cases}\dfrac{1}{N}\displaystyle\sum_{n=0}^{N-1-k}x^{*}(n)x(n+k), & k=0,1,...,p\\ \hat{r}^{*}(-k), & k=(-p+1),(-p+2),...,-1\end{cases} \tag{5}$$

From Eq 4, the estimations of AR parameters can be computed:

$$\hat{a}=-\hat{R}_p^{-1}\hat{r}_p \tag{6}$$

The white noise variance σ^2 is estimated as:

$$\hat{\sigma}^2=\hat{r}(0)+\sum_{k=1}^{p}\hat{a}(k)\hat{r}(-k) \tag{7}$$

Now that the autoregressive parameters have been determined, the PSD of $x(n)$ can be estimated as [31]:

$$\hat{p}(f)=\frac{\sigma^2}{\left|1+\displaystyle\sum_{k=1}^{p}\hat{a}(k)e^{-j2\pi fk}\right|^2} \tag{8}$$

2.3. Zero-phase filter

Filtering manipulations are frequently employed for data processing and analyzing. Although filters are designed primarily according to the amplitude frequency function, great attention should be also paid to the phase frequency function since the phase information of filtered signals is generally distorted after the filtering process. In this study, a zero-phase filtering technique, i.e., the forward--reverse filtering-and-reverse-output (or FRR for short) technique, is adopted to avoid such phase-distortion effects.

The basic idea of conducting a zero-phase filtering process via the FRR method is expressed as follows: (1) the input signal $x(t)$ ($t\in[0,T]$) is firstly filtered via a traditional filter (which is designed according to its amplitude-frequency function) to obtain output $y_1(t)$; (2) $y_1(t)$ is then reversed to produce another sequence $y_2(t)$; (3) $y_2(t)$ is further filtered via the same filter adopted in (1) to generate output $y_3(t)$; (4) $y_2(t)$ is reversed again to get $y_4(t)$. It can be proved that $y_4(t)$ is similar to $y_1(t)$ except that the phase of $y_4(t)$ is not distorted with respect to $x(t)$.

2.4. Random decrement technique

Random decrement technique (RDT) is a time-domain method that uses the ensemble average of output data to approximate the free vibration response of a linear structure that is subjected to Gaussian white noise excitation. The free vibration response is often referred to as a random decrement signature (RDS). This method is based on the assumption that the dynamic response $y(t)$ is a superposition of response components associated respectively with initial displacement $y_{a_0}(t)$, initial velocity $y_{\dot{a}_0}(t)$ and random excitation $y_f(t)$.

The RDT procedure starts with selecting a series of response thresholds $a_{0i}, i=1,2,...,M$ (M), according to which, a sufficient number of segments associated with each value of a_{0i} and meanwhile with the same length can be extracted. These segments are then average so that the response components associated with $y_{\dot{a}_0}(t)$ and $y_f(t)$ can be eliminated, retaining only the component of $y_{a_0}(t)$. The RDS $x(\tau)$ is expressed as [32]:

$$x(\tau) = \frac{1}{N}\sum_{i=1}^{N} y(t_i + \tau) \tag{9}$$

where, τ is the duration (or the length) of the RDS, N is the number of segments involved in the ensemble average.

The logarithmic decrement technique is then used to extract the damping ratio and natural frequency from each of RDSs.

$$x(t) = a_0 \cos(\omega_d t)\cdot \exp(-\zeta\omega_0 t) \tag{10}$$

in which, a_0 is the initial displacement, ω_0 is the circular natural frequency, ω_d is the damped circular natural frequency, and ξ is the damping ratio.

2.5. Bayesian spectral density approach

The BSDA method is a frequency-domain approach for modal identification. It utilizes the statistical properties of the PSD of SDOF response to obtain not only the optimal values of model parameters but also associated estimation uncertainties. The posterior probability density function of modal parameters is constructed by considering the statistical properties of the discrete Fourier transform. Supposing that the excitation can be regarded as a zero-mean white noise process, the PSD of the SDOF response would approximately follow the Chi-square probability distribution. One may then construct a likelihood function of modal parameters to represent the probability of the PSD.

By maximizing the function, or equally by minimizing the logarithm of the function, the optimal estimates of modal parameters can be obtained.

According to the Bayes' theorem, the posterior/updated PDF of the model parameter vector $\theta(\xi, \omega_0, S_{f0})$ is:

$$P(\theta|S_{\ddot{y},N}^{avg}) = K_0 P(\theta) P(S_{\ddot{y},N}^{avg}|\theta) \tag{11}$$

where, K_0 is a non-dimensional constant, $\theta(\xi, \omega_0, S_{f0})$ consists of the damping ratio ξ, natural frequency ω_0 and spectral densities of the modal force S_{f0}, while $P(\theta)$ is the prior PDF of the empirical parameters (determined based on previous knowledge) which can be regarded as a constant in engineering practices. In the above equation, $P(S_{\ddot{y},N}^{avg}|\theta)$ denotes the likelihood function which reflects the contribution of measurements in the posterior PDF. Note that the construction of $P(S_{\ddot{y},N}^{avg}|\theta)$ is a key step in identifying the modal parameters via the Bayesian analysis framework.

Consider the dynamics of a linear SDOF system:

$$\ddot{x} + 2\xi\omega_0\dot{x} + \omega_0^2 x = f(t) \tag{12}$$

where, ξ, ω_0, x are the damping ratio, natural frequency and the displacement response of the oscillator, $f(t)$ is the input excitation which may be regarded as a zero-mean Gaussian white noise process, with its PDF equal to a constant within the concerned frequency range:

$$S_f(\omega) = S_{f0} \tag{13}$$

Assuming that the measured acceleration response of the system $\ddot{y}_n$ is:

$$\ddot{y}_n = \ddot{x}(n\Delta t) + \eta_n \quad (n = 0,1,...,N-1) \tag{14}$$

where, Δt is the sample interval, n indexes the sample number ($0 \le n \le$ N–1), η_n represents noise or errors involved in the measurement, which is also regarded as a zero-mean white noise process. Conventionally, it is assumed that the PSD of η_n, i.e., S_η, is independent to that of $\ddot{x}$:

$$S_\eta = \frac{\Delta t}{2\pi}\sigma_\eta^2 \tag{15}$$

in which, σ_η is the standard deviation of the noise.

The discrete Fourier transform of the stochastic process $\ddot{y}_n$ can be expressed as:

$$\ddot{\gamma}(\omega_k) \equiv \sqrt{\frac{\Delta t}{2\pi N}} \sum_{n=0}^{N-1} \ddot{y}_n \exp(-in\omega_k \Delta t) \tag{16}$$

where, $i = \sqrt{-1}, \Delta\omega = 2\pi / T, T = N\Delta t,\ \omega_k = k\Delta\omega\,(k = 0,..., N_{nqy}),$ with N_{nqy} being an integer nearest to but no larger than half of N.

The PSD of $\ddot{y}_n$ can be then estimated:

$$S_{\ddot{y},N}(\omega_k) = \left|\ddot{\gamma}(\omega_k)\right|^2 = \frac{\Delta t}{2\pi N}\left|\sum_{n=0}^{N-1} \ddot{y} e^{-in\omega_k \Delta t}\right|^2 \tag{17}$$

Accordingly, the mathematical expectation of $S_{\ddot{y},N}$ can be expressed as:

$$\mathrm{E}\left[S_{\ddot{y},N}(\omega_k)\middle|\theta\right] = \mathrm{E}\left[S_{\ddot{x},N}(\omega_k)\middle|\theta\right] + S_\eta \tag{18}$$

with [33]:

$$\mathrm{E}\left[S\ddot{x}(\omega_k)\middle|\theta\right] \approx S\ddot{x}(\omega_k) \tag{19}$$

The PSD of acceleration response of the system subjected to input force $f(t)$ can be deduced as:

$$S_{\ddot{x}}(\omega_k) = \frac{S_f(\omega_k)\omega_k^4}{\left(\omega_0{}^2 - \omega_k{}^2\right)^2 + \left(2\xi\omega_0\omega_k\right)^2} \tag{20}$$

On the other hand, to investigate the statistical properties of $S_{\ddot{y},N}$, $S_{\ddot{y},N}$ can be rewritten in the following form based on Eq 17:

$$S_{\ddot{y},N}(\omega_k) = \xi_c(\omega_k)^2 + \xi_s(\omega_k)^2 \tag{21}$$

with ξ_c and ξ_s denoting the scaled Fourier cosine and sine functions:

$$\begin{aligned} \xi_c(\omega_k) &= \sqrt{\frac{\Delta t}{2\pi N}} \sum_{n=0}^{N-1} \ddot{y}_n \cos(n\omega_k \Delta t) \\ \xi_s(\omega_k) &= \sqrt{\frac{\Delta t}{2\pi N}} \sum_{n=0}^{N-1} \ddot{y}_n \sin(n\omega_k \Delta t) \end{aligned} \tag{22}$$

As $\ddot{y}_n$ belongs to a zero-mean Gaussian stochastic process, so does $\xi_c(\omega_k)$ or $\xi_s(\omega_k)$. Meanwhile, when $\Delta t \to 0^+$, the two random variables $\xi_c(\omega_k)$ and $\xi_s(\omega_k)$ tend to be independent with each other, and the associated variance values become asymptotically equal. Therefore, it follows that the PDF of $S_{\ddot{y},N}(\omega_k)$ can be approximated by a Chi-square distribution.

$$\lim_{\Delta t \to 0^+} S_{\ddot{y},N}(\omega_k) = \frac{1}{2}\left[S_{\ddot{x}}(\omega_k) + S_{\eta}\right]\chi_1 \tag{23}$$

where, χ_1 is the Chi-square distributed with two degrees of freedom.

For $k \neq l$, $S_{\ddot{y},N}(\omega_k)$ and $S_{\ddot{y},N}(\omega_l)$ are uncorrelated in the same frequency segment, and uncorrelated Chi-square random variables should be independent. Thus, for $k,l \in (k_1,k_2)$, $S_{\ddot{y},N} = \left[S_{\ddot{y},N}(k_1\Delta\omega),...,S_{\ddot{y},N}(k_2\Delta\omega)\right]^T$ represents the PSD set in range of $[\omega_{k_1},\omega_{k_2}]$. The joint PDF can be then expressed as:

$$P(S_{\ddot{y},N}|\theta) \approx \prod_{k=k_1}^{k_2} \frac{1}{\mathrm{E}\left[S_{\ddot{y},N}(\omega_k)\right]} \cdot \exp\left\{-\frac{S_{\ddot{y},N}(\omega_k)}{\mathrm{E}\left[S_{\ddot{y},N}(\omega_k)|\theta\right]}\right\} \tag{24}$$

It is worth noting that the frequency range $[\omega_{k1},\omega_{k2}]$ should be selected around a PSD peak of the structural response.

If there are several sets of independent time histories $\ddot{Y} = \left\{\ddot{Y}_N^{(S)}, s = 1,2,...,N_s(N_s \geq N_0)\right\}$, the averaged PSD estimator can be obtained [34]:

$$S_{\ddot{y},N}^{avg}(\omega_k) = \frac{1}{N_s}\sum_{s=1}^{N_s} S_{\ddot{y},N}^{s}(\omega_k) \tag{25}$$

where, N_s is the number of segments, $\ddot{Y}$ represents the time history of output signal, ω_k denotes the frequency which is in range of $[\omega_{k_1},\omega_{k_2}]$.

Thus, the averaged joint PDF can be expressed as:

$$\begin{aligned} P(S_{\ddot{y},N}^{avg}|\theta) = K_1 \prod_{k=k_1}^{k_2} \left|\mathrm{E}\left[S_{\ddot{y},N}(\omega_k)|\theta\right]\right|^{-N_s} \\ \cdot \exp\left[-N_s tr(\left\{\mathrm{E}\left[S_{\ddot{y},N}(\omega_k)|\theta\right]\right\}^{-1} S_{\ddot{y},N}^{avg}(\omega_k))\right] \end{aligned} \tag{26}$$

with K_1 being a constant for a given set of data. Note that K_1 is independent of the modal parameters.

The optimal parameters vector θ^* can be then obtained by maximizing the updated PDF or, equivalently, by minimizing the objective function:

$$g(\theta) = -\ln\left[P(\theta)P(S_{\ddot{y},N}^{avg}|\theta)\right] \tag{27}$$

On the other hand, the uncertainty of identified modal parameters can be quantified by the posterior coefficient of variation (COV) which is defined as the standard deviation of a variable divided by its optimal estimation value [21]. According to the information theory, the standard deviation of each modal parameter is equal to the square of the diagonal element of the inverse matrix of the posteriori covariance matrix, i.e., $\mathrm{H}(\theta^*)^{-1}$, where $\mathrm{H}(\theta^*)$ stands for the Hessian matrix of $g(\theta)$ calculated at [35]:

$$\begin{aligned}\mathrm{H}^{(l,l')}(\theta^*) = \frac{\partial^2 g(\theta)}{\partial\theta_l\partial\theta_{l'}}\Big|_{\theta=\theta^*} = -\frac{\partial^2 \ln[P(\theta)]}{\partial\theta_l\partial\theta_{l'}}\Big|_{\theta=\theta^*} \\ + N_s\sum_{k=k_1}^{k_2}\left[\frac{\partial^2}{\partial\theta_l\partial\theta_{l'}}\left(\ln[|\,\mathrm{E}(S_{\ddot{y},N}(\omega_k)|\theta)\,|] + tr\left\{\frac{S_{\ddot{y},N}^{avg}(\omega_k)}{\mathrm{E}\left[S_{\ddot{y},N}(\omega_k)|\theta\right]}\right\}\right)\right]_{\theta=\theta^*}\end{aligned} \tag{28}$$

where, "tr" stands for the trace of a matrix.

3. Database

As shown in Figure 2a, the studied building is the Leatop Plaza which is located at the urban center of Guangzhou, Guangdong Province of China. This building is of 303 m in height and contains 65 floors above ground. The structural system of the building is composed of a steel diagonal frame and a concrete core tube.

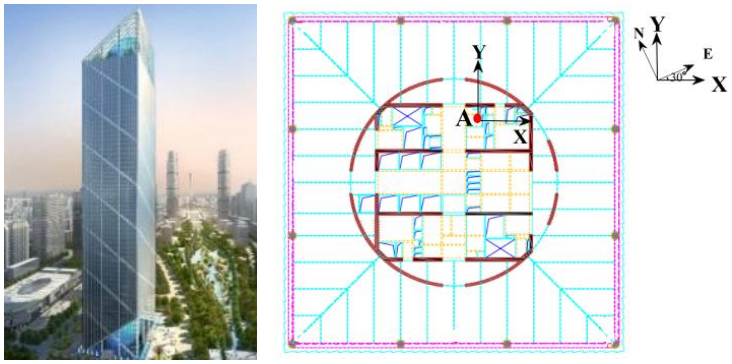

Figure 2. Leatop Plaza and location of accelerometers.

Typhoon Mangkhut is one of the strongest tropical cyclones that have ever influenced Guangzhou. Mangkhut formed over the Northwest Pacific Ocean on September 7, 2018. It landed at the northern part of Philippines with a strength of super typhoon at 1:40 am on September 15. After that, it steered to the South China Sea at a speed of 25 km/h. At 17:00 on September 16, Mangkhut landed at Haiyan Town of Guangdong Province with a maximum sustained wind estimated as 162 km/h (central pressure: 955 hPa). It then weakened rapidly as it moved northwestward continuously until it was finally dissipated. The track of Mangkhut during 16–17 September when the storm influenced the studied building is depicted in Figure 3.

During the passage of Mangkhut, a bi-axial accelerometer was placed at the 56th floor of this high-rise building to measure the wind-induced structural response. The location of the accelerometer is shown in Figure 2(b). Acceleration signals from the accelerometer were first filtered and then recorded at 32 Hz and 64 Hz, respectively. A 30-hr (from 00:00/16 to 06:00/17) database has been collected which covers the whole passage process of Mangkhut around Guangzhou.

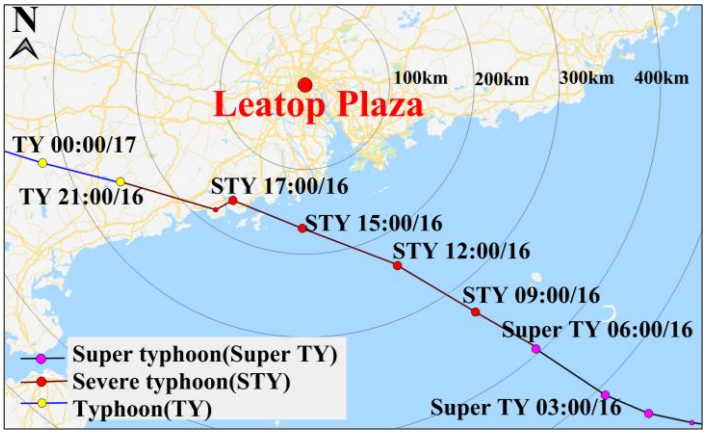

Figure 3. Track of typhoon Mangkhut.

4. Results and discussions

4.1. Acceleration response of the building

Figure 4 illustrates the time histories of measured instantaneous response along the two orthogonal directions. Also depicted are the evolutions of the root-mean-square (RMS) values of each 10-min segment during the passage of Mangkhut. The peak responses along Direction-X were recorded as 2.81 cm/s^2 (instantaneous acceleration) and 1.32 cm/s^2 (RMS), while those along Direction-Y were 5.63 cm/s^2 and 1.83 cm/s^2. Note that the peak responses occurred at ~17:00/16 when Typhoon Mangkhut got closest to the studied building.

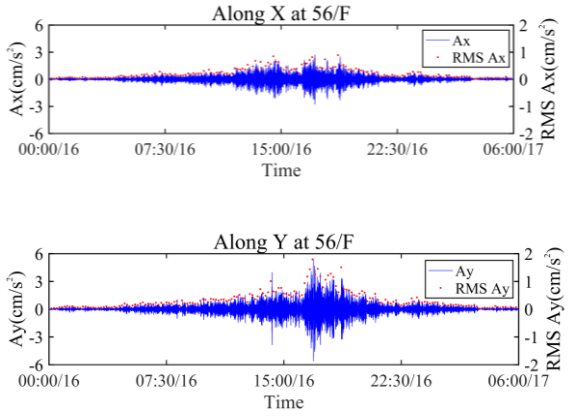

Figure 4. Time history of acceleration response along two orthogonal directions (Ax, Ay) at 56th floor of the building and associated RMS values for each 10-min segment.

4.2. Structural dynamic properties

4.2.1. Optimal estimations of natural frequency and damping ratio

The modal parameters are first determined via the determinist methods. The natural frequencies are identified with the PP method based on the spectral analysis results, while the damping ratios are estimated via the RDT method. Figure 5 exhibits the PSDs of the structural response estimated via both the Welch and Yule-Walker (Yulear) methods from a segment of acceleration data which passed the stationarity test by using the reverse method. As can be seen, results from the two PSD estimation methods show good agreement, and three natural frequencies can be identified in the frequency range below 0.8 Hz. The fundamental natural frequencies are recognized as 0.184 Hz (X-direction) and 0.182 Hz (Y-direction), respectively.

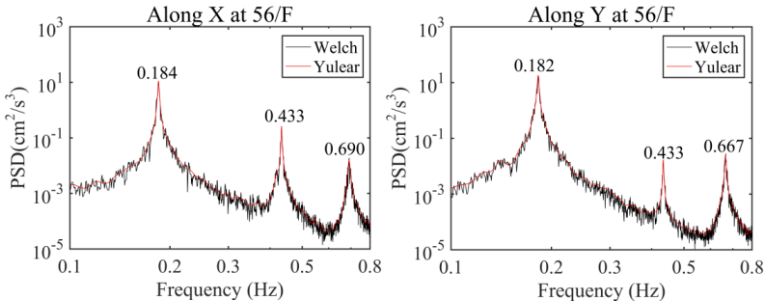

Figure 5. PSD of acceleration responses estimated via Welch and Yule-Walker (Yulear) methods.

Figure 6 plots two typical RDSs. Both the time histories and envelopes of the RDSs are fitted by associated theoretical models to obtain the damping ratio values. The parametric values involved in RDT herein are set in a consistent way to the one adopted in our previous studies [36,37]. The trigger condition (i.e., the initial response of RDS) is set as integer multiples of 0.1σ, σ being the standard deviation of the total response. The length of signature τ is set as a value of 14 times the length of the natural period of concerned mode. For the sake of obtaining damping ratio at high response

amplitudes, the minimum segment number for each RDS is set at a relatively relaxed level of 17. Meanwhile, each obtained RDS has been examined annually to grantee the effectiveness of derived results. As demonstrated, the fitting results agree well with the measured results, with the damping ratios estimated as 0.99% and 0.76% for these two RDSs respectively.

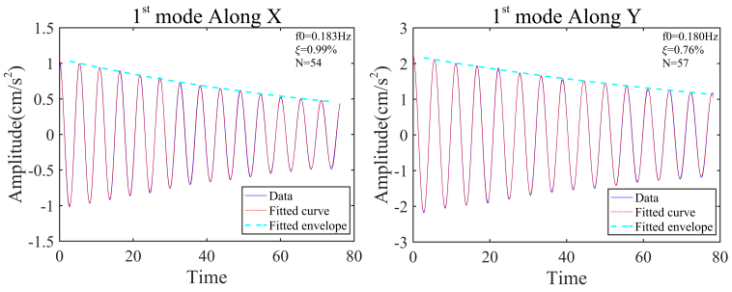

Figure 6. RDSs for 1st mode along two orthogonal directions.

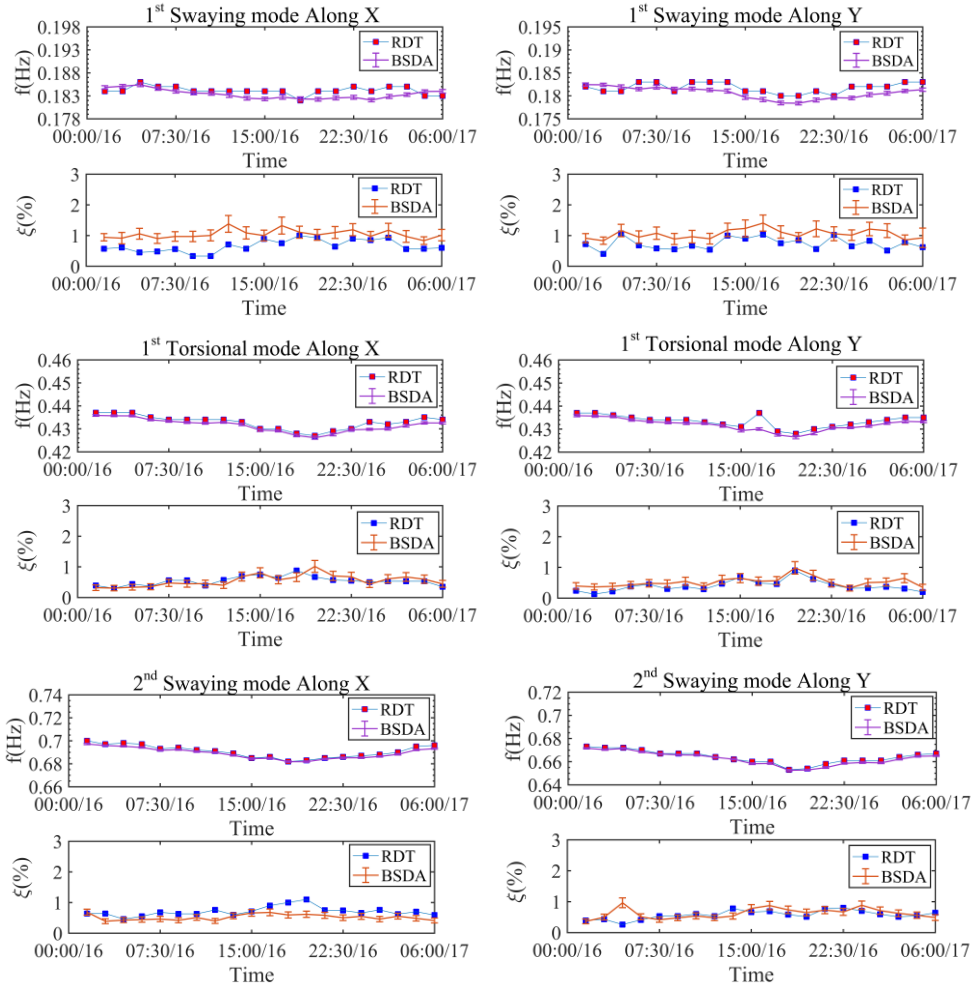

Figure 7. Comparison of modal parameters identified via RDT and BSDA methods for the first two orders of swaying modes and the first torsional mode along two orthogonal directions.

The BSDA method is then applied to estimate the optimal values of modal parameters and corresponding estimation uncertainties. As the wind excitation for the studied building was non-stationary during the passage of the typhoon, the whole dataset is divided into 600 segments (the length of each segment is 3 min), and every ten successive segments (i.e., $N_s = 10$ in equation (28)) are treated as a subset of data for follow-up computations. It is assumed that each subset of data is stationary. Thus, the BSDA method can by adopted properly for modal analysis. It should be pointed out that this assumption is only roughly satisfied for some subsets, which results in estimation errors via the BSDA method. The averaged spectrum $S_{\ddot{y},N}^{avg}(\omega_k)$ for each subset is then calculated and fitted to obtain the optimal estimations of modal parameters. These optimal values are further averaged over every 90-min duration, so that the results can be compared to those obtained via the RDT method which should be exploited on a sufficiently long segment.

Figure 7 plots the identified natural frequencies and damping ratios for the first three orders of modes via the BSDA method against those obtained via the RDT method. It is observed that for higher orders of modes (i.e., 2nd and 3rd modes), the estimations of both natural frequency and damping ratio via these two methods show pretty good agreements. By contrast, the results for the 1st mode demonstrate larger differences. Overall, the optimal values of damping ratio via the BSDA method, which are in range of 0.7%–1.2% (mean value = 0.98%), are found to be ~30% larger than those estimated via RDT which are in range of 0.5%-1.1% (mean value = 0.75%). Even though, the largest relative difference between the two kinds of results for natural frequency is no larger than 2%.

4.2.2. Join PDF of natural frequency and damping ratio

The optimal values of modal parameters can be estimated via the BSDA method for each 3-min segment. Based on these results, the joint PDF of natural frequency and damping over a longer segmental duration can be computed. Figure 8 illustrates the joint PDF of these two parameters estimated from the measurement segment during 17:00/16–18:30/16. The results are compared with the optimal values estimated via the RDT method. Similar to the observations mentioned previously, the damping ratios estimated by RDT for 1st mode are found to be noticeably lower than those via BSDA, while the two kinds of optimal values show good agreement under higher modal order conditions.

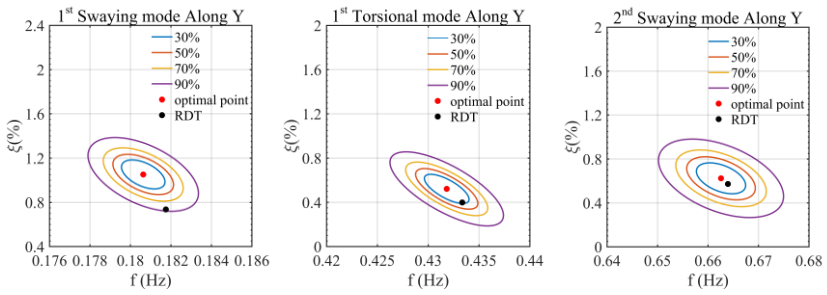

Figure 8. Joint PDF of natural frequency and damping ratio estimated via BSDA overlaid by the result via RDT for the first two orders of swaying modes and the first torsional mode along Direction-Y (the contours describe the confidence intervals of 30%, 50% ,70% and 90% of the marginal updated PDFs).

4.2.3. PSD of modal force identified via BSDA

Figure 9 plots the time histories of identified PSD of modal force S_{f0} (in terms of optimal value and error bands, with each error band corresponding to one standard deviation of the variable away from the optimal value). For reference purpose, the evolutions of 10-min mean wind speed U_{mean} and the peak speed in each 10-min segment U_{peak} are also presented. From these results, the values of S_{f0} varied in a consistent way with wind speed. In addition, the peak value of S_{f0} appeared at the time when Mangkhut got closest to the study site and exerted the strongest wind load on the building.

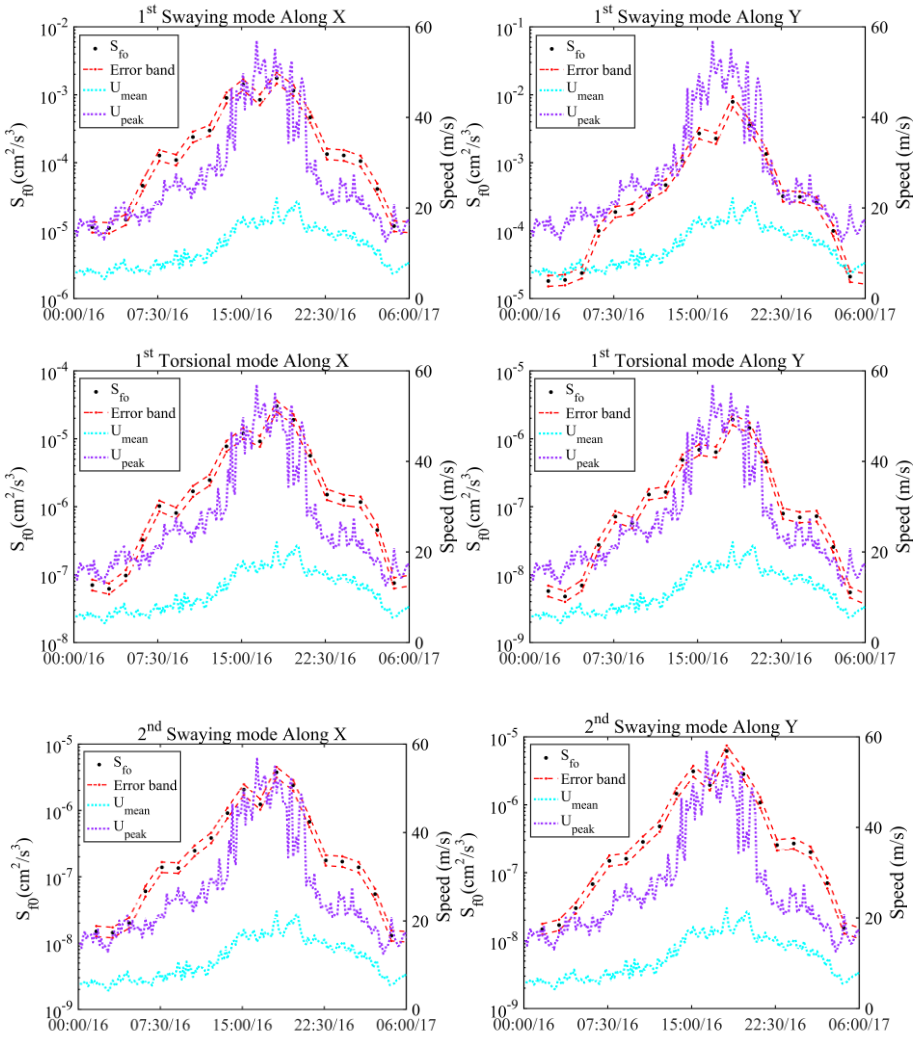

Figure 9. Comparison of time history of identified modal forces (in form of PSD: S_{f0}) via BSDA with measured mean (U_{mean}) and peak (U_{peak}) wind speeds.

4.3. Estimation uncertainty via BSDA

As introduced in the introduction section, there exist many factors in reality (e.g., noise interference, accuracy of experimental instrument and operation method of tests) which can result in evident uncertainty in modal identification results. In order to evaluate the quality of modal analysis results, it is necessary to quantify the estimation uncertainty.

Table 1 illustrates the posterior COV values for each modal parameter identified via the BSDA method. As demonstrated, the maximum COV values for natural frequency f, damping ratio ξ and modal force S_{f0} are 0.21%, 10.08% and 12.00%, respectively. The value for f is much lower than those for S_{f0} and ξ, indicating that the estimation uncertainties for S_{f0} and ξ are comparatively higher than that for f. The above finding may be partially attributed to the large difference between the two kinds of results of ξ estimated respectively via the deterministic method and the BSDA method.

Table 1. Posterior COV of identified modal parameters via BSDA.

COV (%)	X-direction			Y-direction		
	1st swaying mode	1st torsional mode	2nd swaying mode	1st swaying mode	1st torsional mode	2nd swaying mode
f	0.21	0.10	0.08	0.02	0.10	0.08
ξ	7.01	5.31	8.54	6.15	10.08	3.09
S_{fo}	5.60	12.00	8.00	6.40	7.57	9.10

4.4. Serviceability assessment of the building

Occupants may become uncomfortable or even panic when the building is vibrating with excessively large amplitudes. Previous studies have shown that human bodies are more sensitive to the acceleration response of buildings, and the critical levels, exceeding which evident uncomfortable reactions may happen, depend upon frequency. Therefore, a number of frequency-specific criteria have been proposed in terms of acceleration for serviceability assessment of high-rise buildings.

In this paper, four frequency-specific criteria are selected which include the ones stipulated in or proposed by ISO 10137 [38], Melbourne and Palmer [39,40], AIJ-GBV-2004 [41,42], JGJ 3-2010 [43]. All these criteria utilize the peak acceleration response for assessment. As an example, the criterion proposed by Melbourne and Palmer [39,40]is given as follows:

$$\hat{a} = \sqrt{2\ln(f_1 T)}\left(0.68 + \frac{\ln(R)}{5}\right)\exp[-3.65 - 0.41\ln(f_1)] \tag{29}$$

where, f_1 is the fundamental frequency of a building, T is the duration of observation in seconds, R is the return period in years.

It is worth noting that, to take into account the perception discrepancies from different persons, the criterion stipulated in AIJ-GBV-2004 adopts varied critical levels for different percentages of populations [41,42]. Five percentage groups are considered: H-10, H-30, H-50, H-70 and H-90, with the number in each group indicating the perception probability as a percentage. For example, H-10 indicates that 10% of people can perceive the vibration.

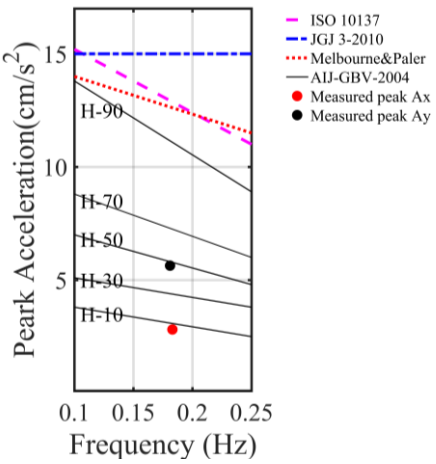

Figure 10. Serviceability assessment of the Leatop plaza against varied frequency-specific comfort criteria (criteria include those documented in ISO 1037 (2007), JGJ 3-2010, Melbourne & Paler (1992), AIJ-GBV-2004; the solid circles stand for the peak structural acceleration responses along the two measurement directions).

Figure 10 illustrates the peak structural response at 56th floor of Leatop Plaza during the passage of Typhoon Mangkhut (2.81 cm/s^2 and 5.63 cm/s^2) against the critical acceleration levels as suggested in the four criteria. It is found that the measured peak acceleration along Direction-y was slightly lower than the H-50 level in AIJ-GBV-2004, and both the peak responses alone the two directions were well below the critical levels suggested by the other three criteria. Therefore, although Typhoon Mangkhut is one of the strongest TCs that have ever impacted Guangzhou, the Leatop Plaza building could work with an acceptable serviceability performance during the passage of this typhoon.

5. Concluding remarks

This paper presents a field study on the modal analysis of a 303 m high-rise building subjected to a landfall typhoon, with a primary objective of comparing the working performance of both a deterministic modal identification method and a Bayesian modal identification approach. The deterministic method is actually a combination of spectral analysis, filtering and random decrement technique (RDT), while the Bayesian method refers to the Bayesian spectral density approach (BSDA).

Through comparison, it is found that for higher orders of modes, the optimal values of natural frequency f and damping ratio ξ estimated via the BSDA method and the adopted deterministic method show good agreements, but the results for 1st mode demonstrate larger differences. Overall,

the optimal values of ξ for 1st mode via BSDA are in a range of 0.7%–1.2%, which are ~30% (the optimal values of damping ratio estimated via the BSDA method are found to be roughly 30% larger than those estimated via RDT) larger than those estimated via RDT (in range of 0.5%-1.1%). Further efforts are needed to clarify the reasons for this discrepancy.

It is stressed that there are two typical advantages by using BSDA against by using the deterministic method: (1) the Bayesian method can be used to estimate the PSD of modal force S_{f0}, but the deterministic method fails to; (2) the Bayesian method can offer uncertainty information of identified modal parameters, which makes it feasible to evaluate the quality of associated estimation results. In this study, S_{f0} is found to vary in a consistent way with wind speed, with its peak values appearing at the time when Mangkhut got closest to the study site and exerted the strongest wind load on the building. On the other hand, the maximum COV values for f, ξ and S_{f0} estimated via BSDA are 0.21%, 10.08% and 12.00%, respectively. The value for f is much lower than those for S_{f0} and ξ, indicating that the estimation uncertainties for the latter two modal parameters are comparatively higher than that for f. It is noted that the COV values of natural frequency and damping ratio are also related to the physical sensitivity of these parameters to loading and external conditions [17,18].

The identified natural frequency is finally utilized for the serviceability assessment of this high-rise building against several frequency-specific criteria. Results show that although Typhoon Mangkhut is one of the strongest TCs that have ever impacted Guangzhou, the Leatop Plaza building could work with an acceptable serviceability performance during the passage of this typhoon.

Acknowledgement

The work described by this paper is supported by two grants from the National Natural Science Foundation of China (Project Nos: 51878194; 51578169). The authors would also like to thank the owners and management officials of the monitored building for the supports during the field test.

Conflict of interest

All authors declare no conflict of interest in this paper.

Reference

1. Q. S. Li, L. H. Zhi, A.Y. Tuan, et al., Dynamic behavior of Taipei 101 tower: Field Measurement and Numerical Analysis, *J. Struct. Eng.*, **137** (2010), 143–155.
2. W. Shi, J. Shan and X. Lu, Modal identification of Shanghai World Financial Center both from free and ambient vibration response, *Eng. Struct.*, **36** (2012), 14–26.

3. H. Akaike, Power spectrum estimation through autoregressive model fitting, *Ann. I. Stat. Math.*, **21** (1969), 407–419.
4. H. A. Cole Jr, On-line failure detection and damping measurement of aerospace structures by random decrement signatures, *NASA Cr-2205: Washington, DC, USA*, (1973).
5. F. Nasser, Z. Li, N. Martin, et al., An automatic approach towards modal parameter estimation for high-rise buildings of multicomponent signals under ambient excitations via filter-free Random Decrement Technique, *Mech. Syst. Signal Proc.*, **70**(2016), 821–831.
6. S. R. Ibrahim and E. C. Mikulcik, A time domain modal vibration test technique, *Shock Vib. Bull.*, **43** (1973), 21–37.
7. J. N. Juang and R. S. Pappa, An eigensystem realization algorithm for modal parameter identification and model reduction, *JGCD.*, **8** (1985), 620–627.
8. B. Peeters and G. De Roeck, Reference-based stochastic subspace identification for output-only modal analysis, *Mech. Syst. Signal Proc.*, **13** (1999), 855-878.
9. G. H. J. Ill, T. G. Carrie and J. P. Lauffer, The Natural Excitation Technique (NExT) for Modal Parameter Extraction from Operating Wind Turbines, *NASA STI/Rec on Technical Report N.*, **93** (1993), 260–277.
10. D. L. Brown, R. J. Allemang, R. Zimmerman, et al., Parameter Estimation Techniques for Modal Analysis, *SAE transactions.*, (1979), 828–846.
11. J. S. Bendat and A. G. Piersol, Engineering applications of correlation and spectral analysis, *New York, Wiley-Interscience.*, (1993), 315.
12. Y. He, Q. Li, H. Zhu, et al., Monitoring of structural modal parameters and dynamic responses of a 600m-high skyscraper during a typhoon, *Struct. Des. Tall Spec. Build.*, **27**(2018), 1456.
13. R. Brincker, L. Zhang and P. Andersen, Modal identification from ambient responses using frequency domain decomposition, Process of the 18th International Modal Analysis Conference, *San Antonio, Texas.*, (2000), 625–630.
14. I. Daubechies, The wavelet transform, time-frequency localization and signal analysis, *IEEE Trans. Inf. Theory.*, **36** (1990), 961–1005.
15. N. E. Huang, Z. Shen, S. R. Long, et al., The empirical mode decomposition method and the Hilbert spectrum for non-stationary time series analysis, *Proc. Roy. Soc. London.*, **454** (1998), 903–995.
16. J. F. Clinton, S. C. Bradford, T. H. Heaton, et al., The observed wander of the natural frequencies in a structure, *Bull Seismol Soc Am.*, **96** (2006), 237–257.
17. R. D. Nayeri, S. F. Masri, R. G. Ghanem, et al., A novel approach for the structural identification and monitoring of a full-scale 17-story building based on ambient vibration measurements, *Smart Mater. Struct.*, **17** (2008), 1–19.
18. A. Mikael, P. Gueguen, P. Y. Bard, et al., The analysis of long-term frequency and damping wandering in buildings using the Random Decrement Technique, *Bull Seismol Soc Am.*, **103** (2013), 236–246.
19. Z. C. Yang, Y. H. Huang, A. R. Liu, et al., Nonlinear in-plane buckling of fixed shallow functionally graded grapheme reinforced composite arches subjected to mechanical and thermal loading, *Appl. Math. Model.*, 70 (2019), 315–327.
20. J. L. Beck and L S. Katafygiotis, Updating Models and Their Uncertainties. I: Bayesian Statistical Framework, *J. Eng. Mech.*, **124** (1998), 455–461.

21. L. S. Katafygiotis, C. Papadimitriou and H. F. Lam, A probabilistic approach to structural model updating, *Soil Dyn. Earthq. Eng.*, **17** (1998), 495–507.
22. L. S. Katafygiotis and K. V. Yuen, Bayes spectral density approach for modal updating using ambient data, *Earthq. Eng. Struct. Dyn.*, **30** (2001), 1103–1123.
23. K. V. Yuen and L. S. Katafygiotis, Bayesian Modal Updating Using Complete Input and Incomplete Response Noisy Measurements, *J. Eng. Mech.*, **128** (2002), 340–350.
24. S. K. Au, Fast Bayesian FFT method for ambient modal identification with separated modes, *J. Eng. Mech.*, **137** (2011), 214–226.
25. S. K. Au, Connecting Bayesian and frequentist quantification of parameter uncertainty in system identification, *Mech. Syst. Signal Proc.*, **29** (2012), 328–342.
26. F. L. Zhang, H. B. Xiong, W. X. Shi, et al., Structural health monitoring of Shanghai Tower during different stages using a Bayesian approach, *Struct. Control. Health Monit.*, **23** (2016), 1366–1384.
27. X. Li and Q. S. Li, Observations of typhoon effects on a high-rise building and verification of wind tunnel predictions, *J. Wind Eng. Ind. Aerodyn.*, **84** (2019), 174–184.
28. S. C. Kuok and K. V. Yuen, Structural health monitoring of Canton Tower using Bayesian framework, *Smart. Struct. Syst.*, **10** (2012), 375–391.
29. Z. Li, M. Q. Feng, L. Luo, et al., Statistical analysis of modal parameters of a suspension bridge based on Bayesian spectral density approach and SHM data, *Mech. Syst. Signal Proc.*, **98** (2018), 352–367.
30. A. Alkan and M. K. Kiymik, Comparison of AR and Welch Methods in Epileptic Seizure Detection, *J. Med. Syst.*, **30** (2006), 413–419.
31. A. Alkan and A. S. Yilmaz, Frequency domain analysis of power system transients using Welch and Yule-Walker AR methods, *Energy Conv. Manag.*, **48** (2007), 2129–2135.
32. W. Shi, J. Shan and X. Lu, Modal identification of Shanghai World Financial Center both from free and ambient vibration response, *Eng. Struct.*, **36** (2012), 14–26.
33. K. V. Yuen and J. L. Beck, Updating properties of nonlinear dynamical systems with uncertain input, *J. Eng. Mech.*, **129** (2003), 9–20.
34. P. R. Krishnaiah, Some recent developments on complex multivariate distributions, *J. Multivariate Anal.*, **6** (1976), 1–30.
35. K. V. Yuen, Bayesian methods for structural dynamics and civil engineering, *Wiley: New York.*, 2010.
36. Y. C. He and Q. S. Li, Dynamic responses of a 492-m-high tall building with active tuned mass damping system during a typhoon, *Struct. Control. Health Monit.*, **21**(2014), 705–720.
37. Z. Li, J. Y. Fu, H. J. Mao, et al., Modal identification of civil structures via covariance-driven stochastic subspace method, *Math. Biosci. Eng.*, **16** (2019), 5709–5728.
38. International Standardization Organization (ISO), Bases for Design of Structures-Serviceability of Buildings and Walkways against Vibrations, *ISO 10137 (2nd Ed.)*, Geneva., 2007.
39. W. H. Melbourne, Probability distributions associated with the wind loading structures, *Civ. Eng. Trans. Inst. Eng. Aust. CE19.*, **1** (1977), 58–67.
40. W. H. Melbourne and T. R. Palmer, Accelerations and comfort criteria for buildings undergoing complex motions, *J. Wind Eng. Ind. Aerodyn.*, **44** (1992), 105–116.

41. Y. Tamura, H. Kawai, Y. Uematsu, et al., Documents for wind resistant design of buildings in Japan. Workshop on Regional Harmonization of Wind Loading and Wind Environmental Specifications in Asia-Pacific Economies (APEC-WW), (2004), 61–84.
42. AL-GBV, Guidelines for the evaluation habitability to building vibration, AIJE-V001-2004, Tokyo, Japan, (2004).
43. JGJ 3-2010. Technical specification for concrete structures of tall building, China Building Industry Press: Beijing, (2010).